A Theoretical Perspective on the Robustness of Feature Extractors

Arjun Nitin Bhagoji [*] [1] **Daniel Cullina** [*] [2] **Ben Y. Zhao** [1]

Abstract

Recent theoretical work on robustness to adversarial examples has derived lower bounds on how robust *any model* can be. However, these bounds do not account for specific models used in practice. In this paper, we develop a methodology to analyze the fundamental limits on the *robustness of fixed feature extractors*, which in turn provides bounds on the robustness of classifiers trained on top of them. The tightness of these bounds relies on the effectiveness of the method used to find collisions between pairs of perturbed examples at deeper layers. For linear feature extractors, we provide closed-form expressions for collision finding while for piece-wise linear feature extractors, we propose a bespoke algorithm based on the iterative solution of a convex program that provably finds collisions. We utilize our bounds to identify structural features of classifiers that lead to a lack of robustness and provide insights into the effectiveness of different training methods at obtaining robust feature extractors.

1. Introduction

Determining lower bounds on the robustness of classifiers to adversarial examples has emerged as an important problem to understand both how effective specific classifiers are (Bunel et al., 2017; Tjeng et al., 2019; Gowal et al., 2018) and what non-trivial regimes for learning *any classifier* in the presence of adversarial examples are (Pydi & Jog, 2020; Bhagoji et al., 2019; 2021). Lower bounds have allowed a move away from the attack-defense arms race (Madry et al., 2018; Zhang et al., 2019; Croce & Hein, 2020) to an understanding of how robust classifiers can be, in more general settings.

[*]Equal contribution [1]Department of Computer Science, University of Chicago [2]School of Electrical Engineering and Computer Science, Pennsylvania State University. Correspondence to: Arjun Nitin Bhagoji <abhagoji@uchicago.edu>.

2^{nd} *AdvML Frontiers workshop at* 40^{th} *International Conference on Machine Learning*, Honolulu, Hawaii, USA. PMLR 202, 2023. Copyright 2023 by the author(s).

In this paper, we turn our focus to determining *lower bounds on the robustness of feature extractors*. An understanding of how robust a given feature extractor is important for two reasons. First, it sheds light on the impact of common architectural choices, such as activation functions and dimensionality reduction, on robustness. Second, it allows for an informed choice between different feature extractors in learning paradigms such as transfer and semi-supervised learning. Our work also bridges the aforementioned approaches which focused at one end on certifying the robustness of specific classifiers and at the other on information-theoretic bounds applicable only to the set of all classifiers. We determine lower bounds on fixed feature extractors by answering the following key question:

What is the minimum robust loss incurred by any classifier trained on top of a fixed feature extractor?

Collision-finding for lower bound determination: To determine classifier-agnostic lower bounds on robustness, earlier work focused on the interaction between points from different classes in the input space when perturbed through the construction of a *conflict graph*. Minimizing an appropriately defined loss function over this graph determines an information-theoretic lower bound on the loss. Intuitively, the denser the graph is, the higher the lower bound. Finding these collisions for features extracted from a non-convex feature extractor, like a neural network, is the non-trivial technical task we address in this paper.

Our **contributions** in this paper are:

Lower bounds on robustness for fixed feature extractors (Section 2): We extend prior work by providing a method to derive lower bounds on all classifiers that use a fixed feature extractor. We construct a distance function over the input space that depends on the feature extractor in use. This method applies to all discrete data distributions, adversary neighborhood contraints and fixed feature extractors.

Novel algorithm for collision finding (Section 3): To construct the conflict graph needed to determine lower bounds, we propose new algorithms for efficiently finding collisions between adversarially-modified features. We find these to be critical due to the ineffectiveness of existing algorithms such as Projected Gradient Descent at finding collisions. For *linear feature extractors* such as the first layer of a neural network, we determine exact, closed form expressions to find collisions. For *non-linear feature extractors*, specifically piece-wise linear ones (such as ReLU layers), we develop a descent algorithm that solves a sequence of convex optimization problems over polytopes.

Empirical findings (Section 4): We utilize our method to find numerical lower bounds on the robustness of fixed feature extractors trained on the MNIST and Fashion MNIST datasets. Our results show that both dimensionality-reducing linear layers as well as the information loss induced by ReLU activations can lead to significantly less robust networks. We also found that, at certain layers, TRADES (Zhang et al., 2019) led to somewhat less robust feature extractors than standard adversarial training (Madry et al., 2018). We discuss the implications of our bounds for the design of better robust models in Section 5.

2. Lower bounds for fixed feature extractors

In this section, we develop a method for evaluating the robustness of a feature extractor for classification in the presence of a test-time adversary. We characterize the optimal adversarial loss achievable by any classifier that uses the fixed feature extractor as its initial layer. Our method applies for any discrete data distribution, non-empty neighborhood constraint, and a fixed, measurable feature extractor.

2.1. Background

Examples and labels: We consider a supervised classification problem with a test-time adversary. We have an example space $\mathcal{X}$ and a label space $\mathcal{Y} = \{-1, 1\}$. Labeled examples are sampled from a joint probability distribution P over $\mathcal{X} \times \mathcal{Y}$.

Test-time adversary: The test-time adversary modifies a natural example subject to some constraints to generate an adversarial example that will be classified (Goodfellow et al., 2015; Szegedy et al., 2013; Carlini & Wagner, 2017). Formally, the adversary samples a labeled example (x, y) from P and selects $\tilde{x} \in N(x)$, where $N : \mathcal{X} \to 2^{\tilde{\mathcal{X}}}$ is the neighborhood function encoding the constraints on the adversary and $\tilde{\mathcal{X}}$ is the space of adversarial examples.[1] For all x, $N(x)$ must be nonempty. This definition encompasses the ℓ_p family of constraints widely used in previous work.

Measuring adversarial loss: We consider 'soft' classification functions (or classifiers) that map examples to probability distributions over the classes. These are $h : \mathcal{X} \to \Delta^{\mathcal{Y}}$, where $\Delta^{\mathcal{Y}} = \{p \in \mathbb{R}^{\mathcal{Y}} : p \geq \mathbf{0}, \sum_{y \in \mathcal{Y}} p_y = 1\}$. We measure classification performance with a loss function $\ell : \Delta^{\mathcal{Y}} \times \mathcal{Y} \to \mathbb{R}$, so the expected performance of a classifier h is $\mathbb{E}[\sup_{\tilde{x} \in N(x)} \ell(h(\tilde{x}), y)]$, where $(x, y) \sim P$. In the two class setting, $h(\tilde{x})_{-1} = 1 - h(\tilde{x})_1$, so any loss function that treats the classes symmetrically can be expressed as $\ell(p, y) = \ell'(p_y)$. Additionally, ℓ' should be decreasing. Together, these allow the optimization over adversarial examples to be moved inside the loss function, giving $\mathbb{E}\left[\ell\left(\inf_{\tilde{x} \in N(x)} h(\tilde{x})_y, y\right)\right]$. Thus, the adversarial optimization can be analyzed by itself.

[1] In most but not all previously studied settings, $\tilde{\mathcal{X}} = \mathcal{X}$. Making the distinction helps to clarify some of our definitions and affects what properties they can be expected to have.

2.2. Extending to fixed feature extractors

Definition 1. *For a soft classifier h, the correct-classification probability q_v that it achieves on an example $v = (x, y)$ in the presence of an adversary is $q_v = \inf_{\tilde{x} \in N(x)} h(\tilde{x})_y$. The space of achievable correct classification probabilities is $\mathcal{P}_{\mathcal{V},N,\mathcal{H}} \subseteq [0, 1]^{\mathcal{V}}$, defined as $\mathcal{P}_{\mathcal{V},N,\mathcal{H}} = \bigcup_{h \in \mathcal{H}} \prod_{(x,y) \in \mathcal{V}} \left[0, \inf_{\tilde{x} \in N(x)} h(\tilde{x})_y\right]$.*

(Bhagoji et al., 2021) characterized $\mathcal{P}_{\mathcal{V},N,\mathcal{H}}$ in the case that $\mathcal{H}$ is the class of measurable functions $\mathcal{X} \to \Delta^{\mathcal{Y}}$. For a data distribution P that is discrete with finite support $\mathcal{V} \subseteq \mathcal{X} \times \mathcal{Y}$, this allows the minimum adversarial loss achievable to be expressed as an optimization over $\mathcal{P}_{\mathcal{V},N,\mathcal{H}}$:

$$\inf_{h \in \mathcal{H}} \mathbb{E}_{(x,y) \sim P}\left[\sup_{\tilde{x} \in N(x)} \ell(h(\tilde{x}), y)\right] = \inf_{q \in \mathcal{P}_{\mathcal{V},N,\mathcal{H}}} \sum_{v \in \mathcal{V}} P(\{v\}) \ell'(q_v).$$

We extend their approach to analyze feature extractors as follows. Given a feature space $\mathcal{Z}$ and a *fixed, measurable feature extractor* $f : \tilde{\mathcal{X}} \to \mathcal{Z}$, define $\mathcal{H}_f = \{h \in \mathcal{H} : h = g \circ f\}$: an element of $\mathcal{H}_f$ is some measureable $g : \mathcal{Z} \to \Delta^{\mathcal{Y}}$ composed with f. Our aim is to characterize $\mathcal{P}_{\mathcal{V},N,\mathcal{H}_f}$ so that we can optimize loss functions over it to evaluate the suitability of f.

Conflict graph: In (Bhagoji et al., 2021), the notion of a conflict graph was used to record neighborhood intersections for pairs of points from different classes. When such an intersection exists, it is impossible for any classifier to correctly classify both of those points in the adversarial setting. We extend this notion to apply to the family of classifiers using a fixed feature extractor f. In our setting, a conflict exists between a pair of points when each of them has a neighbor that is mapped to the same point in the feature space.

We call the conflict graph $G_{\mathcal{V},N,f}$, where $\mathcal{V} \subseteq \mathcal{X} \times \mathcal{Y}$. When we apply $G_{\mathcal{V},N,f}$ in order to understand classification of labeled examples with distribution P, we take $\mathcal{V}$ to be the support of P. The graph is bipartite: the vertex set is partitioned into parts $\mathcal{V}_c = \mathcal{V} \cap (\mathcal{X} \times \{c\})$. The edge set is $\mathcal{E}_{\mathcal{V},N,f} \subseteq \mathcal{V}_1 \times \mathcal{V}_{-1}$ and it contain the edge $((u, 1), (v, -1))$ when there is some $\tilde{u} \in N(u)$ and some $\tilde{v} \in N(v)$ such that $f(\tilde{u}) = f(\tilde{v})$.

Lemma 1 (Feasible output probabilities)**.** *The set of cor-*

rect classification probability vectors for support points $\mathcal{V}$, adversarial constraint N, and hypothesis class $\mathcal{H}_f$ is

$$\mathcal{P}_{\mathcal{V},N,\mathcal{H}_f} = \{q \in \mathbb{R}^{\mathcal{V}} : q \geq \mathbf{0},\, q \leq \mathbf{1}, Bq \leq \mathbf{1}\} \qquad (1)$$

where $B \in \mathbb{R}^{\mathcal{E}\times\mathcal{V}}$ is the edge incidence matrix of the conflict graph $G_{\mathcal{V},N,f}$.

The proof is given in Appendix A.

Approximating $G_{\mathcal{V},N,f}$ and $\mathcal{P}_{\mathcal{V},N,\mathcal{H}_f}$: If instead of knowing the true conflict graph $G_{\mathcal{V},N,f}$, we have some subgraph, then we can find a polytope that is a superset of the true $\mathcal{P}_{\mathcal{V},N,\mathcal{H}_f}$. If we minimize some expected loss over this proxy polytope, we obtain a lower bound on the optimal loss over H_f. Because subgraphs of the conflict graph lead to valid lower bounds on optimal classification performance, we can use this method to evaluate the quality of a feature extractor f even if exact computation of the conflict graph is computationally intractable.

2.3. Distance interpretation

In the most commonly studied settings, the neighborhood constraint arises from a distance function: $N_\varepsilon(x) = \{\tilde{x} \in \tilde{\mathcal{X}} : d(x,\tilde{x}) \leq \varepsilon\}$. This parameter ε is the adversarial budget constraint. For any two examples u and v, a natural quantity to consider is $\varepsilon^*(u,v) = \inf\{\varepsilon \geq 0 : N_\varepsilon(u) \cap N_\varepsilon(v) \neq \varnothing\}$, the smallest adversarial budget that would cause the edge (u,v) be appear in the conflict graph. We will call this the distance on $\mathcal{X}$ induced by d. The following equivalent expression is useful for computing the distance: $\varepsilon^*(u,v) = \inf_{\tilde{x}\in\tilde{\mathcal{X}}} \max(d(u,\tilde{x}), d(v,\tilde{x}))$. When $\mathcal{X} = \tilde{\mathcal{X}} = \mathbb{R}^d$ and $d(x,x') = \|x - x'\|_p$, the minimal adversarial budget is simply $\frac{1}{2}\|u - v\|_p$. This definition generalizes easily to the setting of classification with a particular feature extractor, but the resulting quantity is much more interesting.

Definition 2. *The distance induced on $\mathcal{X}$ by d and f is the minimum adversarial budget required to create a conflict between u and v after a feature extractor f:*

$$\begin{aligned}\varepsilon_f^*(u,v) &= \inf\{\varepsilon \geq 0 : f(N_\varepsilon(u)) \cap f(N_\varepsilon(v)) \neq \varnothing\},\\ &= \inf_{\tilde{u},\tilde{v}\in\tilde{\mathcal{X}}: f(\tilde{u})=f(\tilde{v})} \max(d(u,\tilde{u}), d(v,\tilde{v})). \qquad (2)\end{aligned}$$

This reduces to $\varepsilon^*(u,v)$ when f is the identity function, or more generally any injective function. Any choice of $\tilde{u}$ and $\tilde{v}$ in (2) provides an upper bound on $\varepsilon_f^*(u,v)$, which is useful for finding a subgraph of $G_{\mathcal{V},N,f}$ and a lower bound on optimal classification performance in $\mathcal{H}_f$.

Induced distance is not a distance on the feature space: The fact ε_f^* is defined on $\mathcal{X}$ is essential: it is not possible to interpret it as a distance on $\mathcal{Z}$. For a full explanation of this point, see Appendix B.

3. Distance computations for practical feature extractors

In this section, we provide algorithms to find collisions between the features resulting from adversarially perturbed data. Lower bounds for specific datasets and architectures are in Section 4. For brevity, the single-layer version of the algorithms are presented in this Section, with the general algorithm described in Appendix C.

We now describe the concrete setting that we will work in for the remainder of the paper. We assume that our example space is a real vector space and that adversarial examples are from the same space: $\mathcal{X} = \tilde{\mathcal{X}} = \mathbb{R}^{n_1}$. Let $\mathcal{B} \subseteq \mathcal{X}$ be a nonempty, closed, convex, origin-symmetric set. These conditions imply the zero vector in contained in $\mathcal{B}$. We take the neighborhood of any point to be a scaled, shifted version of this ball: $N_\varepsilon(x) : x + \varepsilon\mathcal{B}$. Neighborhood constraints derived from ℓ_p ($p \geq 1$) norms fit into this class: by defining $\mathcal{B} = \{\delta \in \mathbb{R}^{n_1} : \|\delta\|_p \leq 1\}$, we obtain $N_\varepsilon(x) = \{\tilde{x} \in \mathbb{R}^{n_1} : \|\tilde{x} - x\|_p \leq \varepsilon\}$. We will focus on ℓ_2-based neighborhoods, but our algorithms can work for any choice of $\mathcal{B}$ over which efficient optimization is possible.

3.1. Linear feature extractors

Suppose that our feature extractor is an affine linear function of the input example: $f(x) = Lx + k$ for some matrix $L \in \mathbb{R}^{n_2\times n_1}$ and vector $k \in \mathbb{R}^{n_2}$. Then the distance $\varepsilon_f(u,v)$ becomes

$$\inf\{\varepsilon \geq 0 : (k + L(u + \varepsilon\mathcal{B})) \cap (k + L(v + \varepsilon\mathcal{B})) \neq \varnothing\}.$$

Because $\{(\varepsilon,\delta) \in \mathbb{R}^{1+n_1} : \delta \in \varepsilon\mathcal{B}\}$ is closed convex cone, $\varepsilon_f(u,v)$ can be expressed as the following convex optimization problem (ConeLP):

$$\inf \varepsilon \quad \text{subject to } \delta \in \varepsilon\mathcal{B},\ \delta' \in \varepsilon\mathcal{B},\ L(\delta - \delta') = L(v - u).$$

Because $\mathcal{B}$ is closed and the linear subspace is always nonempty, the infimum is achieved. Also, it is sufficient to consider (δ,δ') satisfying $\delta' = -\delta$: for any feasible $(\varepsilon,\delta,\delta')$, the point $(\varepsilon, (\delta-\delta')/2, (\delta'-\delta)/2)$ is also feasible, has the same value, and satisfies the additional constraint. The feasibility of the symmetrized point uses the origin-symmetry of $\mathcal{B}$. The simplified program is

$$\min \varepsilon \quad \text{subject to } \delta \in \varepsilon\mathcal{B}, \quad L\delta = L(v - u)/2.$$

Thus the optimal adversarial strategy for creating conflict between u and v is intuitive: produce examples with the same features as the midpoint $(u + v)/2$.

Explicit expressions with ℓ_2 constaints: If $\mathcal{B}$ is the unit ℓ_2 ball, there are further simplifications. Consider the singular value decomposition $L = U\Sigma V^T$ where we do not include zero singular values in Σ. Then the linear map given by $U\Sigma$

is injective and can be canceled from the linear constraint on δ. The resulting program is

$$\min \varepsilon \text{ subject to } \|\delta\|_2 \le \varepsilon, \quad V^T\delta = \frac{1}{2}V^T(v-u),$$

the optimal choice of δ is $\delta = \frac{1}{2}VV^T(v-u)$, and $\varepsilon_f(u,v) = \frac{1}{2}\|V^T(v-u)\|_2$. Observe that this is the norm of a vector in $\mathbb{R}^{n_2}$, i.e. the feature space, contrasting with our discussion in Section B. However, this is essentially the only case $\varepsilon_f(u,v)$ simplifies into a feature space distance.

3.2. Fully connected networks with ReLU activations

For this architecture, we have $f = f^{(\ell)} \circ \ldots \circ f^{(1)}$ where the layer i function is $f^{(i)} : \mathbb{R}^{n_i} \to \mathbb{R}^{n_{i+1}}$, $f^{(i)}(z) = (k^{(i)} + L^{(i)}z)^+$. Here z^+ represents the component-wise positive part of the vector z. Then $\varepsilon_f(u,v)$ is the value of the following optimization problem:

$$\min \varepsilon \quad \text{subject to } \delta \in \varepsilon\mathcal{B},\ \delta' \in \varepsilon\mathcal{B}, f(u+\delta) = f(v+\delta').$$

As in the linear case, the minimum exists because the cones are closed and the equality constraint is feasible. In contrast with the linear case, the equality constraint is nonconvex.

Linear pieces of f: The local linear approximation to $f^{(i)}(z)$ around a point z' is $\operatorname{diag}(s^{(i,z')})(k^{(i)} + L^{(i)}z)$, where $s^{(i,z')}$ is a zero-one vector that depends on the sign pattern of $k^{(i)} + L^{(i)}z'$: $s_j^{(i,z')} = \mathbf{1}((k^{(i)} + L^{(i)}z')_j > 0)$. In other words, $s^{(i,z')}$ is the ReLU activation pattern at layer i when z' is the input to that layer.

Using these linear approximations, the feasible set of $(\delta, \delta') \in \mathbb{R}^{n_1+n_1}$ satisfying the constraint $f(u+\delta) = f(v+\delta')$ can be decomposed as a union of polytopes: each activation pattern defines a linear subspace and there are some linear inequalities specifying the region where that activation pattern actually occurs. For a one-layer network, the linear piece for pattern s is

$$f(z) = \operatorname{diag}(s)(k+Lz) \ \text{ for } \ \operatorname{diag}(2s-1)(k+Lz) \ge 0.$$

Thus one of the polytopes composing the feasible set is $(\delta, \delta') \in \mathbb{R}^{n_1+n_1}$ satisfying

$$\begin{aligned}
&\operatorname{diag}(s)(k+L(u+\delta)) = \operatorname{diag}(s')(k+L(v+\delta')),\\
&(2\operatorname{diag}(s) - I)(k+L(u+\delta)) \ge 0,\\
&(2\operatorname{diag}(s') - I)(k+L(v+\delta')) \ge 0.
\end{aligned}$$

In the one-layer case, the whole feasible region is covered by polytopes where $s = s'$. Observe that the dimension of the subspace satisfying the linear equality varies with s. When f contains multiple layers, each polytope in the feasible set is defined by a linear equality constraint involving feature vectors together with a linear inequality for the sign of each ReLU input.

Algorithm 1 The single layer versions of the descent algorithm with midpoint initialization and the linear cone program. We have $u, v, \delta, \delta' \in \mathbb{R}^{n_1}$, $k, w, s, z, z' \in \mathbb{R}^{n_2}$, $L \in R^{n_2 \times n_1}$, and $\varepsilon \in \mathbb{R}$.

```
1:  FINDCOLLISION($u, v, L, k$)
2:      $w \leftarrow k + \frac{1}{2}L(u+v)$, $\varepsilon \leftarrow \frac{1}{2}\|u-v\|$
3:      for $0 \le j < n_2$ do $s_j \leftarrow \mathbf{1}(w_j > 0)$
4:      repeat
5:          $\varepsilon^{\text{old}} \leftarrow \varepsilon$
6:          $(\varepsilon, \delta, \delta', z, z') \leftarrow$ CONELP($L, u, v$)
7:          $s^{\text{old}} \leftarrow s$
8:          for $0 \le j < n_2$ do
9:              if $z_j > 0$ and $z'_j > 0$ then
10:                 $s_j \leftarrow 1 - s_j$
11:     until $s^{\text{old}} = s$ or $\varepsilon^{\text{old}} = \varepsilon$
12:     return $\varepsilon, \delta, \delta'$
```

Descent algorithm: We optimize over this feasible set with a descent algorithm: Algorithm 1 details the version for single-layer networks. The method generalizes to multiple layers and is used to obtain our results in Section 4.2. A full description of the general version is in Appendix C. We initialize our search in a polytope that we know to be nonempty: the one containing the feature space collision induced by the midpoint of the two examples. Within a polytope, we minimize the objective exactly by solving a linear cone program. We examine the dual variables associated with the linear inequality constraints to determine whether an adjacent polytope exists in which we can continue the search.

We need not just the values of the primal solution, but the values of dual variables associated with the linear inequalities in the solution to the dual problem. These are called z and z' in Algorithm 1. When both $z_j > 0$ and $z'_j > 0$, the input to ReLU j is zero when both $f(u+\delta)$ and $f(v+\delta')$ are computed, and the objective function could be decreased further by allowing the input to switch signs. In this case, we move to another polytope based on the new ReLU states and search there.

When we fail to find such pairs of dual variables, either the minimum is in the interior of the current polytope (and thus is supported only by cone constraints), or the minimum is on the boundary of the current polytope but there is no adjacent polytope in which we could continue the search. Thus we end the search.

Algorithm termination, convergence, and complexity: The descent algorithm will terminate in a finite number of iterations and will find a local minimum of the distance function. Since the feasible space is non-convex, any local descent procedure is not guaranteed to find the global minimum. The number of variables in the cone program

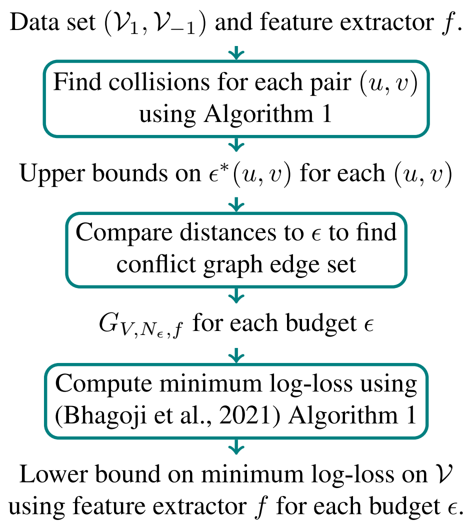
Data set $(\mathcal{V}_1, \mathcal{V}_{-1})$ and feature extractor f.
Find collisions for each pair (u, v) using Algorithm 1
Upper bounds on $\epsilon^*(u, v)$ for each (u, v)
Compare distances to ϵ to find conflict graph edge set
$G_{V,N_\epsilon,f}$ for each budget ϵ
Compute minimum log-loss using (Bhagoji et al., 2021) Algorithm 1
Lower bound on minimum log-loss on $\mathcal{V}$ using feature extractor f for each budget ϵ.

Figure 1. Pipeline for experimental evaluations.

is proportional to the number of ReLUs in the feature extractor plus the dimension of the example space. The time-complexity of a single iteration of the search is *polynomial in the input dimension and number of ReLUs.* The feasible region is the union of a finite but exponentially large number of convex polytopes. Due to the requirement that each iteration make progress, it is impossible to ever revisit a polytope. Thus, *termination is guaranteed*, but no polynomial bound on the number of iterations is available. We suspect that as in the case of the simplex algorithm for linear programming, input data resulting in an extremely large number of iterations may exist, but would have a delicate structure that is unlikely to arise in practice. Other common layers are discussed in

4. Evaluation

In this section, we put into practice the methodology outlined in the previous sections for determining the robustness of a fixed feature extractor (see Figure 1).

4.1. From collision-finding to lower bounds

Vertices $\mathcal{V}$ from training data: The vertex set $\mathcal{V}$ is a representation of the training data. We use 2-class problems derived from MNIST (LeCun & Cortes, 1998) or Fashion MNIST (Xiao et al., 2017) as in previous work (Pydi & Jog, 2020; Bhagoji et al., 2019; 2021).

Neighborhood function N: We use the common ℓ_2-norm constraint (Madry et al., 2018), in which the adversary's strength is parametrized by the radius ϵ of the ball.

Fixed feature extractors f: We use the composition of the layers of convolutional and fully-connected DNNs as our fixed feature extractors (details in Appendix F). The linear part of the first layer behaves as a linear feature extractor. Subsequent layers behave as non-linear feature extractors. These networks are trained using either CE loss minimization or robust training with either adversarial training (Madry et al., 2018) or TRADES (Zhang et al., 2019).

Edge set $\mathcal{E}$ from collision finding: Algorithm 1 [2] provides a greedy, iterative method to find collisions between feature representations of pairs of points from different classes. Each successful collision is an edge in the bipartite conflict graph. Each iteration of this algorithm can be cast as a convex program in the form of a linear cone (as detailed in Appendix D). We solve this linear cone program using CVXOPT (Andersen et al., 2013). Since we are working with an ℓ_2-norm constrained adversary, we can speed up computation by projecting the inputs onto the space spanned by the right singular vectors of the first linear layer. For linear convolutional layers, we cast the convolution operation as a matrix multiplication to enable the use of the closed form derived in Section 3.1.

Computing the lower bound from the conflict graph: The conflict graph determines the set of possible output probabilities for each vertex (training data point) for the optimal classifier. Minimizing the $0-1$ and cross-entropy losses over this graph thus results in a lower bound over these losses since any classifier must incur a larger loss than the optimal classifier, by definition. We use the method from (Bhagoji et al., 2021) over the conflict graphs we derive from deeper layer representations. Results in the main body are for the cross-entropy loss (others in Appendix H).

4.2. Results

Interpreting the results: In all of our plots, we show the lower bound on all measurable classifiers for a given dataset and adversarial budget obtained from (Bhagoji et al., 2021) (labeled *Input space*). Our bounds for fixed feature extractors should be compared to this lower bound, which represents the best possible performance for any classifier. The magnitude of the difference provides a qualitative measure of that subset of features' contribution to the overall network's lack of robustness.

How does robustness evolve across layers? For both benign and robust models (Fig. 2), fixing the first linear layer immediately leads to a jump in the lower bound on robustness. This indicates that the representations after the first linear layer as not as 'well-separated' as in the input space. We find that the first ReLU activation layer contributes significantly to an increase in the lower bound for both benign and robustly trained networks. We observe that post-ReLU representations tend to be sparse, leading to an easier search

[2]We experimented with a modification of the Auto-PGD (Croce & Hein, 2020) algorithm to find collisions at deeper layers with fixed budgets. This was far less effective at finding collisions, so all results use Alg. 1.

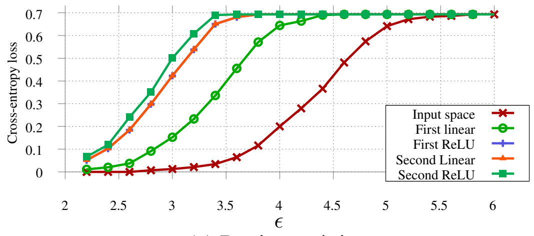

(a) Benign training

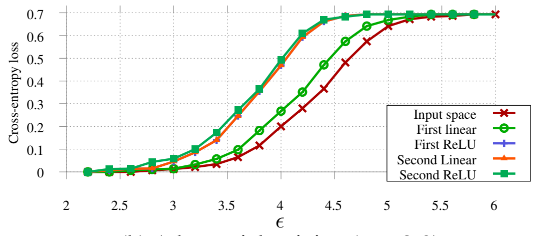

(b) Adversarial training ($\epsilon = 2.0$)

Figure 2. Robustness of representations obtained from different layers of 3-layer FCNNs on MNIST

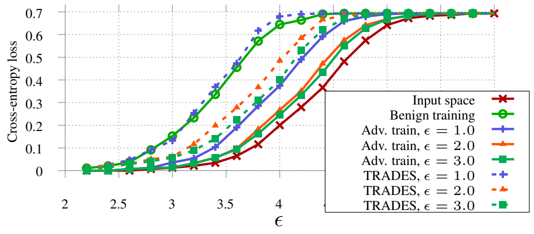

(a) First Linear

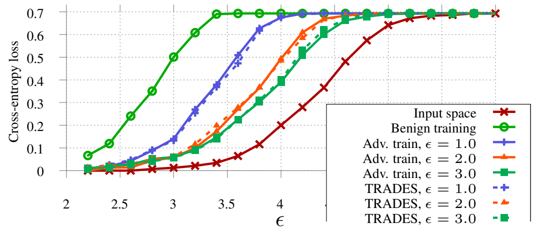

(b) Second ReLU

Figure 3. Robustness of the representations obtained from a 3-layer FCNN on MNIST using different training procedures

problem and a larger number of collisions. The second linear layer, on the other hand, does not lead to much additional increase in the loss. This is a property of the particular architecture we use, and a smaller linear layer is likely to lead to larger increases in loss. Finally, the second set of ReLU activations does have a measurable impact on robustness, particularly for the benign network. Appendix H.2 shows that decreasing the width of feature extractors leads to a drop in robustness.

How does the parametrization of robust training impact layer-wise robustness? Linear layers of models with benign training are the least robust, with robustness increasing with the budget ϵ_{train} used during training. This trend holds for deeper layers in the model as well, with features extracted from robustly trained networks being more robust than their benign counterparts for corresponding values of ϵ. We find a significant difference between PGD-based adversarial training and TRADES in terms of the robustness of their first linear layers (Fig. 3), but this largely disappears by the second ReLU activation layer. Interestingly, the marginal benefits of using a larger budget reduce as ϵ_{train} increases. Further, we observe a phenomenon where layers of a network robustly trained using higher values of ϵ_{train} can be *less* robust than those using a lower value.

5. Discussion

Implications for training robust models: Our results indicate that layers in the network that reduce the effective dimension of their incoming inputs have the largest negative impact on robustness (see further results in Appendix H.2). Two prominent examples of this are ReLU layers that reduce effective dimension by only considering non-negative outputs and fully connected layers with fewer outputs than inputs. On the other hand, linear convolutional layers do not have a negative impact on robustness. This indicates that not reducing the effective dimension of any deeper feature to be lower than that of the input data is likely to benefit robustness. Further, our results confirm that the use of larger values of ϵ_{train} does not necessarily translate to higher robustness at lower budgets. This indicates the need to be robust to more than a single adversary at a time. Finally, we find a qualitative difference in the layers learned using PGD-training and TRADES, implying interesting learning dynamics with different robust losses.

Extending to state-of-the-art models and datasets: All of our experiments in this paper are on simple models and datasets which demonstrate the feasibility and use of our method. However, state-of-the art feature extractors for datasets such as Imagenet are far deeper than those considered in this paper. Thus, our algorithm would need to be made considerably faster to handle these cases. While our framework, can handle skip connections, networks with attention are beyond its scope. Nevertheless, the feature extractors we consider *are robust* for the tasks we evaluate them on, making our results and conclusions representative.

Acknowledgements

ANB and BYZ were supported in part by NSF grants CNS-1949650, CNS-1923778, CNS-1705042, the C3.ai DTI, and the DARPA GARD program. DC was supported in part by the C3.ai DTI. Any opinions, findings, and conclusions or recommendations expressed in this material are those of the author(s) and do not necessarily reflect the views of the funding agencies.

References

Andersen, M., Dahl, J., and Vandenberghe, L. Cvxopt: Python software for convex optimization, 2013.

Bhagoji, A. N., Cullina, D., and Mittal, P. Lower bounds on adversarial robustness from optimal transport. In *Advances in Neural Information Processing Systems*, pp. 7496–7508, 2019.

Bhagoji, A. N., Cullina, D., Sehwag, V., and Mittal, P. Lower bounds on cross-entropy loss in the presence of test-time adversaries. In *ICML*, 2021.

Bunel, R., Turkaslan, I., Torr, P. H., Kohli, P., and Kumar, M. P. A unified view of piecewise linear neural network verification. *arXiv preprint arXiv:1711.00455*, 2017.

Carlini, N. and Wagner, D. Towards evaluating the robustness of neural networks. In *Security and Privacy (SP), 2017 IEEE Symposium on*, pp. 39–57. IEEE, 2017.

Cohen, J., Rosenfeld, E., and Kolter, Z. Certified adversarial robustness via randomized smoothing. In *International Conference on Machine Learning*, pp. 1310–1320. PMLR, 2019.

Croce, F. and Hein, M. Reliable evaluation of adversarial robustness with an ensemble of diverse parameter-free attacks. In *International Conference on Machine Learning*, pp. 2206–2216. PMLR, 2020.

Dohmatob, E. Generalized no free lunch theorem for adversarial robustness. In *Proceedings of the 36th International Conference on Machine Learning*, pp. 1646–1654, 2019.

Goodfellow, I. J., Shlens, J., and Szegedy, C. Explaining and harnessing adversarial examples. In *International Conference on Learning Representations*, 2015.

Gowal, S., Dvijotham, K., Stanforth, R., Bunel, R., Qin, C., Uesato, J., Mann, T., and Kohli, P. On the effectiveness of interval bound propagation for training verifiably robust models. *arXiv preprint arXiv:1810.12715*, 2018.

Kolter, J. Z. and Wong, E. Provable defenses against adversarial examples via the convex outer adversarial polytope. In *ICML*, 2018.

LeCun, Y. and Cortes, C. The MNIST database of handwritten digits. 1998.

Li, L., Qi, X., Xie, T., and Li, B. Sok: Certified robustness for deep neural networks. *arXiv preprint arXiv:2009.04131*, 2020.

Madry, A., Makelov, A., Schmidt, L., Tsipras, D., and Vladu, A. Towards deep learning models resistant to adversarial attacks. In *ICLR*, 2018.

Mahloujifar, S., Diochnos, D. I., and Mahmoody, M. The curse of concentration in robust learning: Evasion and poisoning attacks from concentration of measure. In *Proceedings of the AAAI Conference on Artificial Intelligence*, volume 33, pp. 4536–4543, 2019.

Pydi, M. S. and Jog, V. Adversarial risk via optimal transport and optimal couplings. In *Proceedings of the 37th International Conference on Machine Learning*, pp. 7814–7823, 2020.

Raghunathan, A., Steinhardt, J., and Liang, P. Certified defenses against adversarial examples. In *ICLR*, 2018.

Szegedy, C., Zaremba, W., Sutskever, I., Bruna, J., Erhan, D., Goodfellow, I., and Fergus, R. Intriguing properties of neural networks. *arXiv preprint arXiv:1312.6199*, 2013.

Tjeng, V., Xiao, K. Y., and Tedrake, R. Evaluating robustness of neural networks with mixed integer programming. In *ICLR*, 2019.

Xiao, H., Rasul, K., and Vollgraf, R. Fashion-mnist: a novel image dataset for benchmarking machine learning algorithms, 2017.

Zhang, H., Yu, Y., Jiao, J., Xing, E., Ghaoui, L., and Jordan, M. Theoretically principled trade-off between robustness and accuracy. In *ICML*, 2019.

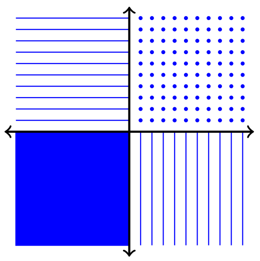
(a) Some fibers of f

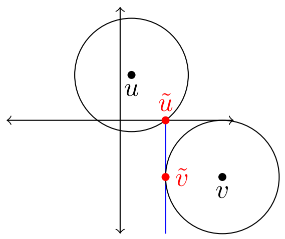

(b) $\varepsilon_f^*(u,v)$ with $f^{-1}(\tilde{z})$

Figure 4. Induced distances for $f : \mathbb{R}^2 \to \mathbb{R}^2$, $f(x_0,x_1) = (\max(x_0,0), \max(x_1,0))$, (a pair of ReLUs). Let $a, b > 0$. Then the fiber $f^{-1}(\{(a,b)\})$ is the point $\{(a,b)\}$. The fiber $f^{-1}(\{(a,0)\})$ is the ray $\{(a,y) : y \le 0\}$. The fiber $f^{-1}(\{(0,0)\})$ is the quadrant $\{(x,y) : x \le 0, y \le 0\}$. For $u = (1,4)$ and $v = (9,-5)$, we have $\varepsilon_f^*(u,v) = 5$, $\tilde{u} = (4,0)$, $\tilde{v} = (4,-5)$, and $\tilde{z} = f(\tilde{u}) = f(\tilde{v}) = (4,0)$.

A. Proofs

Proof of Lemma 1. Suppose that $e = ((u,1),(v,-1)) \in \mathcal{E}$. Then, there are some $\tilde{z} \in \mathcal{Z}$, $\tilde{u} \in N(u)$, and $\tilde{v} \in N(v)$ such that $f(\tilde{u}) = f(\tilde{v}) = \tilde{z}$. We have $q_u \le h(f(\tilde{u}))_1 = h(\tilde{z})_1$, $q_v \le h(f(\tilde{v}))_{-1} = h(\tilde{z})_{-1}$, and $h(\tilde{z})_1 + h(\tilde{z})_{-1} = 1$. Combining these gives the constraint $(Bq)_e \le 1$, which appears in (1).

Now, we will show that each vector q in the polytope is achievable by some h. The construction is simple: at each point in the feature space, assign the largest possible probability to class 1: let $h(\tilde{z})_1 = \sup_{w : \tilde{z} \in f(N(w))} q_w$ and $h(\tilde{z})_{-1} = 1 - h(\tilde{z})_1$. This achieves the desired performance for examples from class 1:

$$\inf_{\tilde{u} \in N(u)} h(f(\tilde{u}))_1 = \inf_{\tilde{u} \in N(u)} \sup_{w : f(\tilde{u}) \in f(N(w))} q_w \ge \inf_{\tilde{u} \in N(u)} q_u = q_u.$$

For an example is v in class -1 we have

$$\begin{aligned}
\inf_{\tilde{v} \in N(v)} h(f(\tilde{v}))_{-1} &= \inf_{\tilde{v} \in N(v)} \left(1 - \sup_{w : f(\tilde{v}) \in f(N(w))} q_w\right) \\
&= \inf_{\tilde{v} \in N(v)} \inf_{w : f(\tilde{v}) \in f(N(w))} (1 - q_w) \\
&= \inf_{w : ((w,1),(v,-1)) \in \mathcal{E}} (1 - q_w) \\
&\ge q_v.
\end{aligned}$$

The final inequality uses the fact that q satisfies $Bq \le \mathbf{1}$. □

B. Induced distance is not a distance on $\mathcal{Z}$

Figure 4 illustrates the computation of ε_f^* for a simple f that is related to the ReLU function.

The fact ε_f^* is defined on $\mathcal{X}$ is essential. It is not possible to interpret the induced distance as a distance in the feature space $\mathcal{Z}$. This is because $f(N_\varepsilon(x))$, the set of features of points near x, cannot be derived from $f(N_0(x))$, the set of features of the uncorrupted version of x. This is because distinct choices of x may lead to the same features $f(N_0(x))$, but f may vary more in the neighborhood of one choice of x that the other.

An example is helpful to illustrate this point. Let $\mathcal{X} = \tilde{\mathcal{X}} = \mathbb{R}^2$, let $\mathcal{Z} = \mathbb{R}$, let $N_\varepsilon(x)$ be the closed ℓ_2 ball of radius ε around x, and let $f(x_0,x_1) = \arctan(x_1/x_0)$ for $x \ne 0$ (the value that we pick for $f(0,x_1)$ is irrelevant). In other words, f finds the angle between the horizontal axis and the line containing x. The range of values that the adversary can cause $f(\tilde{x})$ to take depends on $\|x\|$. If $\|x\|_2 < \varepsilon$, $f(\tilde{x})$ can be any angle from 0 to π, and if $\|x\|_2 \ge \varepsilon$, $|f(\tilde{x}) - f(x)| \le \arcsin(\varepsilon/\|x\|_2)$.

This example also illustrates that ε_f is not necessarily a metric, even in cases where d is a metric. Given $u, v \in \mathbb{R}^2$, we have $\varepsilon_f(u,\alpha u) = 0$, $\varepsilon_f(u,\alpha u) = 0$, and $\varepsilon_f(\alpha u, \alpha v)$ can be made arbitrarily small by selecting α to be small. Despite this, $\varepsilon(u,v)$ will be on the order of $\min(\|u\|,\|v\|)$.

An alternative approach to studying the induced distance is to define an adversarial classification problem on $\mathcal{Z}$ by taking $N_\varepsilon^{\mathcal{Z}}(z) = f(N_\varepsilon(f^{-1}(\{z\})))$. Note that this construction only makes sense when $\mathcal{X} = \tilde{\mathcal{X}}$ and thus the domain of f is $\mathcal{X}$. This is more conservative: for any feature point z it considers the worst-case x with feature z: the x in whose neighborhood f varies the most.

C. Descent algorithm for multiple layer networks

We start by repeating the notion used in Section 3.2: $f = f^{(\ell)} \circ \ldots \circ f^{(1)}$ where the layer i function is $f^{(i)} : \mathbb{R}^{n_i} \to \mathbb{R}^{n_{i+1}}$, $f^{(i)}(z) = (k^{(i)} + L^{(i)} z)^+$. Then $\varepsilon_f(u, v)$ is the value of the following optimization problem:

$$\min \varepsilon \quad \text{subject to } \delta \in \varepsilon\mathcal{B}, \quad \delta' \in \varepsilon\mathcal{B}, \quad (f^{(\ell)} \circ \ldots \circ f^{(1)})(u + \delta) = (f^{(\ell)} \circ \ldots \circ f^{(1)})(v + \delta').$$

Using the local linear approximation, the equality constraint becomes

$$\begin{aligned}\operatorname{diag}(s^{(\ell)})(k^{(\ell)} + L^{(\ell)}(\ldots \operatorname{diag}(s^{(1)})(k^{(1)} + L^{(1)}(u + \delta)))) \\ = \operatorname{diag}(s'^{(\ell)})(k^{(\ell)} + L^{(\ell)}(\ldots \operatorname{diag}(s'^{(1)})(k^{(1)} + L^{(1)})(v + \delta')))).\end{aligned}$$

and for each $1 \le i \le \ell$, the inequalities

$$\begin{aligned}(2 \operatorname{diag}(s^{(i)}) - I)(k^{(i)} + L^{(i)}(\ldots \operatorname{diag}(s^{(1)})(k^{(1)} + L^{(1)}(u + \delta)))) \ge 0 \\ (2 \operatorname{diag}(s'^{(i)}) - I)(k^{(i)} + L^{(i)}(\ldots \operatorname{diag}(s'^{(1)})(k^{(1)} + L^{(1)}(v + \delta')))) \ge 0\end{aligned}$$

must hold in order for the linear approximation to be valid. Any collision must be in a polytope with $s^{(\ell)} = s'^{(\ell)}$, which is why we only needed one set of s variables in the single layer case. However, ReLU activation variables for earlier layers cannot be merged.

The main modification to algorithm is to the process of changing the s variables after each iteration. The variables for all but the final layer are allowed to change independently, while the variables in the final layer are changed together following the same rule as in the single layer algorithm.

Algorithm 2 Descent with midpoint initialization

```
Require: $u, v \in \mathbb{R}^{n_1}$, $L \in R^{n_2 \times n_1}$, $k \in \mathbb{R}^{n_2}$
Ensure: $\varepsilon \in \mathbb{R}$, $\delta, \delta' \in \mathbb{R}^{n_1}$
1: $z \leftarrow k + \frac{1}{2}L(u+v)$, $\varepsilon \leftarrow \frac{1}{2}\|u-v\|$
2: for $0 \le j < n_2$ do
3:     $s_j \leftarrow \mathbf{1}(z_j > 0)$,
4: end for
5: repeat
6:     $\varepsilon^{\text{old}} \leftarrow \varepsilon$
7:     $(\varepsilon, \delta, \delta', z, z') \leftarrow$ ConeLP($L^{(1)} \dots L^{(\ell)}, k^{(1)} \dots k^{(\ell)}, u, v, s^{(1)} \dots s^{(\ell)}, s'^{(1)} \dots s'^{(\ell-1)}$)
8:     $s^{\text{old}} \leftarrow s$
9:     for $1 \le i \le \ell - 1$ do
10:        for $0 \le j < n_{i+1}$ do
11:            if $z_j^{(i)} > 0$ then
12:                $s_j^{(i)} \leftarrow 1 - s_j^{(i)}$
13:            end if
14:            if $z_j'^{(i)} > 0$ then
15:                $s_j'^{(i)} \leftarrow 1 - s_j'^{(i)}$
16:            end if
17:        end for
18:    end for
19:    for $0 \le j < n_{\ell+1}$ do
20:        if $z_j^{(\ell)} > 0$ and $z_j'^{(\ell)} > 0$ then
21:            $s_j^{(\ell)} \leftarrow 1 - s_j^{(\ell)}$
22:        end if
23:    end for
24: until $s^{\text{old}} = s$ or $\varepsilon^{\text{old}} = \varepsilon$
```

D. Converting collision finding to a linear cone program

In this section, we demonstrate how the collision finding problem after one linear and one ReLU layer can be cast as a linear cone program.

We have a network with first layer $v \mapsto Lv + k$ where $L \in \mathbb{R}^{n_1 \times n_0}$ and $k \in \mathbb{R}^{n_1}$.

Given a pair of points $(v', v'') \in \mathbb{R}^{2n_0}$ we would like to search over the space of $(\delta', \delta'') \in \mathbb{R}^{2n_0}$ such that $(L(v'+\delta')-k)^+ = (L(v''+\delta'')-k)^+$. This space is always nonempty because we can take $v'+\delta' = v''+\delta'' = (v'+v'')/2$.

Let $S \subseteq [n_1]$ be the subset of active ReLUs. Let $F \in \mathbb{R}^{|S| \times n_1}$ be the inclusion indicator matrix for the subset: $F_{i,j} = 1$ if and only if $j \in S$ and $|S \cap [j]| = i$ (there are exactly i elements of S strictly smaller than j, so j is the $i+1$st element of S). Let D be the diagonal matrix with $D_{j,j} = 1$ for $j \in S$ and $D_{j,j} = -1$ for $j \notin S$.

For $j \in S$ (the active ReLUs), we need the constraint $(L(v'+\delta')+k)_j = (L(v'+\delta')+k)_j$. In matrix form, this is $FL(v'+\delta') = FL(v''+\delta'')$,

For $j \in S$, we need $(L(v'+\delta')+k)_j \ge 0$, $(L(v''+\delta'')+k)_j \ge 0$, and for $j \notin S$, we need $(L(v'+\delta')+k)_j \le 0$, $(L(v''+\delta'')+k)_j \le 0$. In matrix form, these are $D(L(v'+\delta')+k) \ge 0$, $D(L(v''+\delta'')+k) \ge 0$.

Our objective is $\max(\|\delta'\|_2, \|\delta''\|_2)$. We will replace with a linear objective by adding two additional variables (t', t'') satisfying $t' \ge \|\delta'\|_2$ and $t'' \ge \|\delta''\|_2$.

The cvx-opt system is

$$\begin{aligned} &\text{minimize } c^T x \\ &\text{subject to } Gx + s = h \\ &\qquad\qquad Ax = b \\ &\qquad\qquad s \succeq 0 \end{aligned}$$

The cones involved are a nonnegative orthant of dimension $2n_1$ and two second order cones, each of dimension $n_0 + 1$. Thus $s = (D(L(v' + \delta') + k), D(L(v'' + \delta'') + k), t', \delta', t'', \delta'')$. We then let $x = (t, \delta', \delta'')$. The matrix relating s and x is $G \in \mathbb{R}^{(n_1+n_1+1+n_0+1+n_0)\times(1+n_0+n_0)}$ and $s = h - Gx$. The block structure is

$$G = \begin{pmatrix} 0 & -DL & 0 \\ 0 & 0 & -DL \\ -1 & 0 & 0 \\ 0 & -I & 0 \\ -1 & 0 & 0 \\ 0 & 0 & -I \end{pmatrix} \qquad h = \begin{pmatrix} D(Lv' + k) \\ D(Lv'' + k) \\ 0 \\ 0 \\ 0 \\ 0 \end{pmatrix}$$

We use $Ax = b$ to encode $FL(\delta' - \delta'') = -FL(v' - v'')$, so $A \in \mathbb{R}^{|S|\times(1+n_0+n_0)}$, $b \in \mathbb{R}^{|S|}$, and

$$A = \begin{pmatrix} 0 & FL & -FL \end{pmatrix} \qquad b = -FL(v' - v'').$$

Finally,

$$c = \begin{pmatrix} 1 \\ 0 \\ 0 \end{pmatrix}.$$

D.1. Factorized L

If $n_1 < n_0$, then we can take advantage of the fact that the rank of L is at most n_1. Let $L = U\Sigma V^T$.

Replace $L(v + \delta)$ with $U\Sigma(V^T v + \epsilon)$, n_0 with size of Σ.

New G and A:

$$G = \begin{pmatrix} 0 & -DU\Sigma & 0 \\ 0 & 0 & -DU\Sigma \\ -1 & 0 & 0 \\ 0 & -I & 0 \\ -1 & 0 & 0 \\ 0 & 0 & -I \end{pmatrix}$$
$$A = \begin{pmatrix} 0 & FU\Sigma & -FU\Sigma \end{pmatrix}$$

Also, the length of c is reduced. The constant vectors h and b are unchanged.

E. Further common layers

Batch-normalization: Batch norm layers are simply affine functions of their inputs at test-time, and the transformations they induce can be easily included in a linear layer.

Max pooling: Max-pool layers, like ReLUs, are piecewise linear functions of their inputs, so constraints coming from the equality of max-pool outputs also lead to feasible regions that are the union of polytopes. This is a simple extension left for future work due to a lack of space.

Other activation functions and architectures: Injective activation functions such as Leaky ReLU, ELU and sigmoid will not lead to additional collisions. Further, since they are not piecewise linear, a different descent algorithm would be needed. Our framework cannot find collisions in networks with both forward and backward flows, such as attention.

F. Further experimental details

We consider the following two architectures for our experiments:

1. 3-layer fully connected neural network (FCNN): 300 FC-ReLU-200 FC-ReLU-2 FC
2. 4-layer convolutional neural network (CNN): 20$\times$5$\times$5 conv.-BN-ReLU- 2$\times$2 MaxPool-50$\times$5$\times$5 conv.-BN-ReLU-2$\times$2 MaxPool- 500 FC - 2 FC

We also construct a 'Small' and 'Smaller' version of the FCNN with layers that are $2\times$ and $4\times$ narrower respectively.

G. Related Work

Related work on robustness lower bounds: When the data distribution satisfies certain properties, (Dohmatob, 2019) and (Mahloujifar et al., 2019) use the 'blowup' property to determine bounds on the robust loss, given some level of loss on benign data. We note that these papers use a different loss function that depends on the original classification output on benign data, thus their bounds are not comparable. (Bhagoji et al., 2019), (Pydi & Jog, 2020) and (Bhagoji et al., 2021) provide lower bounds on robust loss when the set of classifiers under consideration is all measurable functions. These bounds are classifier-agnostic and do not depend on the loss on benign data.

Related work on certification and verification: Work on certified robustness has considered techniques for training neural networks such that the resulting models are provably robust to perturbations upper bounded by a given budget (Kolter & Wong, 2018; Raghunathan et al., 2018; Cohen et al., 2019; Li et al., 2020). Typically, these models can only be certified to be robust to small budgets. In contrast, our work provides lower bounds on the robustness of partial models which are applicable across a large range of budgets. Approaches to verifying the robustness of neural networks (Bunel et al., 2017; Tjeng et al., 2019; Gowal et al., 2018) are closely related to our work, but differ in that they consider fixed end-to-end networks while we focus on a layer-by-layer analysis, allowing us to argue about the robustness of classifiers trained on top of given feature extractors.

H. Additional Results

H.1. Impact of linear convolutional layers on robustness

As discussed in Section **??**, the first convolutional layer can be thought as simply a matrix multiplication, although the size of the resulting matrix can be large. We find that since the effective dimension of the resulting features is much larger than the input dimension for the datasets we consider, the linear convolutional layer does not lead to an increase in the lower bound (Fig. 12 in Appendix).

H.2. Impact of reduction of network size

In Figure 7, we compare the robustness of representations obtained from fully connected networks with decreasing layer sizes. The 'Regular' network is the one used throughout, while the 'Small' and 'Smaller' networks have corresponding layers that are $2\times$ and $4\times$ narrower respectively. We can clearly see that as the width of the feature extractor decreases, so does its robustness.

H.3. $0-1$ Loss results

In Figures 8, 9, 10 and 11 we provide lower bounds on the $0-1$ loss in the same settings as those considered in the main body of the paper. We note that the results and conclusions remain the same qualitatively.

H.4. Linear convolutional layers

In Figure 12, we can see that the representations extracted from the first linear layer of a convolutional network do not have any negative impact on the robustness of the overall model.

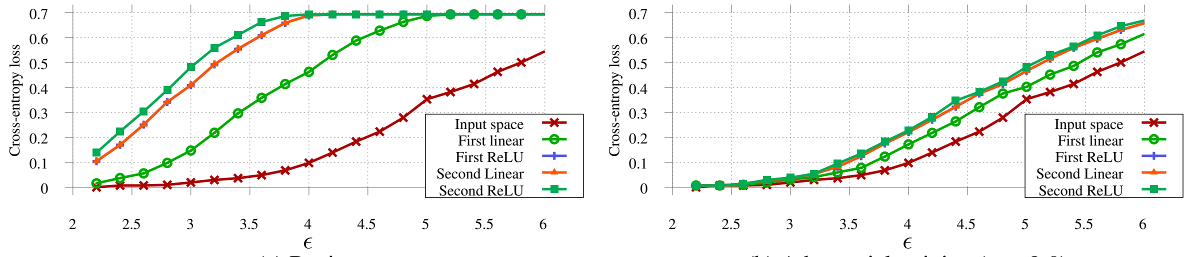

(a) Benign (b) Adversarial training ($\epsilon = 2.0$)

Figure 5. Robustness of representations obtained from different layers of a 3-layer FCNN trained using benign training on Fashion MNIST

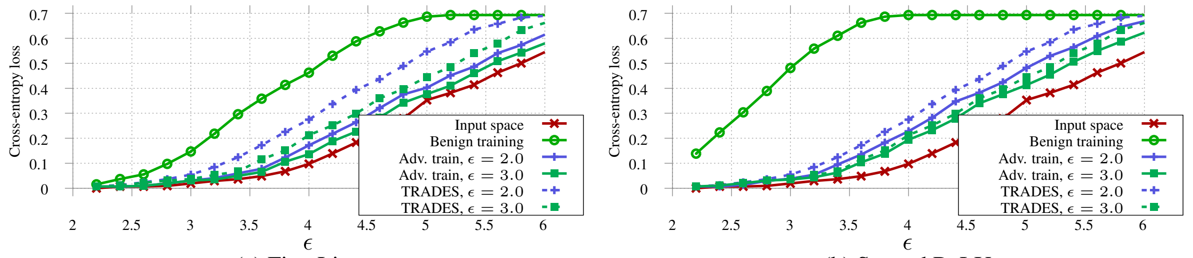

(a) First Linear (b) Second ReLU

Figure 6. Robustness of the representations obtained from a 3-layer FCNN using different training procedures on Fashion MNIST

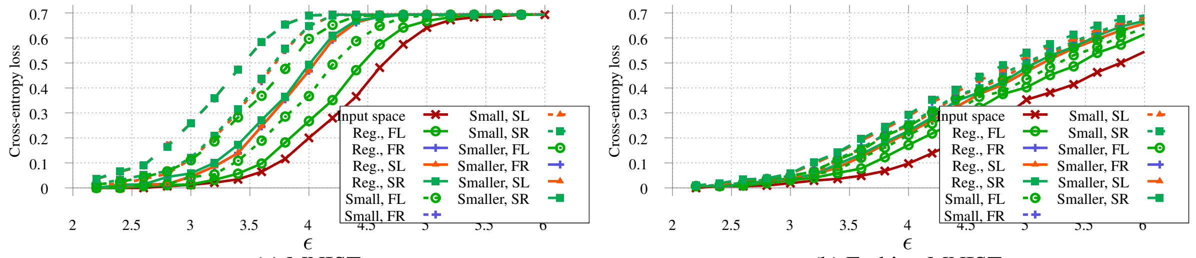

(a) MNIST (b) Fashion MNIST

Figure 7. Robustness of the representations obtained from fully connected networks with layers of decreasing size.

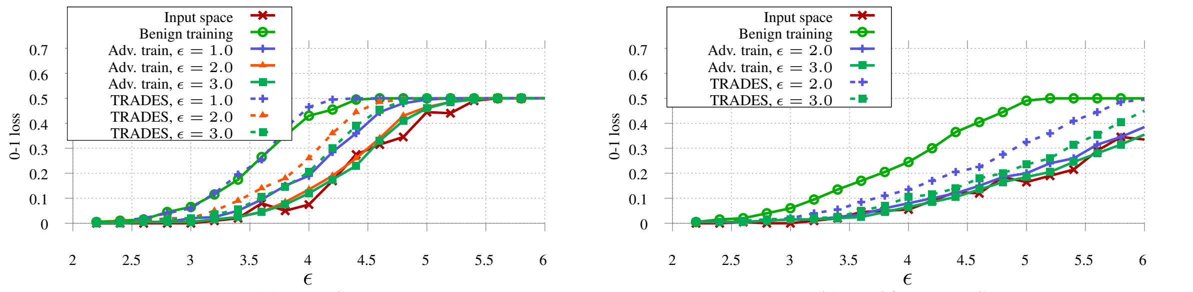

(a) MNIST (b) Fashion MNIST

Figure 8. $0 - 1$ Loss: Robustness of the representation obtained from the *first linear layer* of a 3-layer FCNN using different training procedures

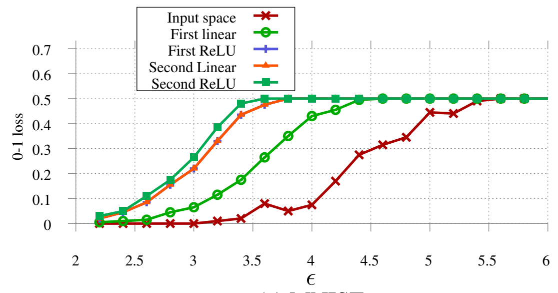

(a) MNIST

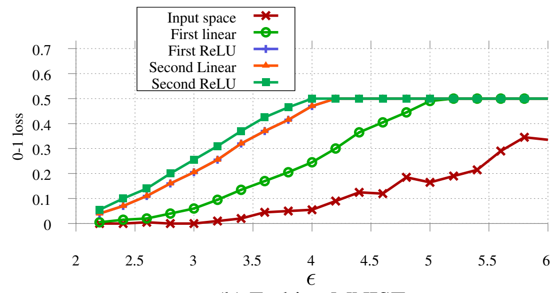

(b) Fashion MNIST

Figure 9. $0-1$ Loss: Robustness of representations obtained from different layers of a 3-layer FCNN trained using benign training

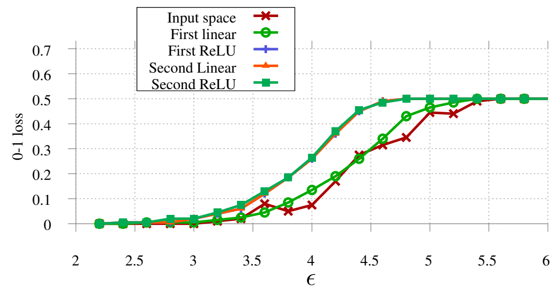

(a) MNIST

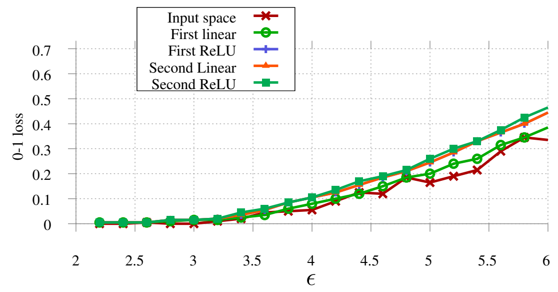

(b) Fashion MNIST

Figure 10. $0-1$ Loss: Robustness of representations obtained from different layers of a 3-layer FCNN trained using PGD adversarial training with $\epsilon = 2.0$

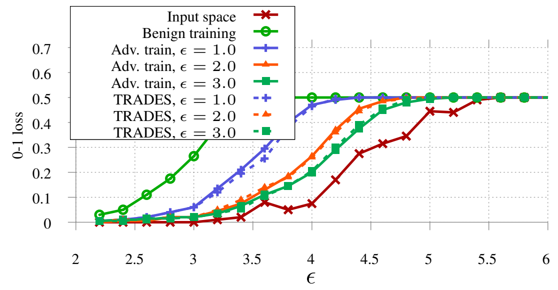

(a) MNIST

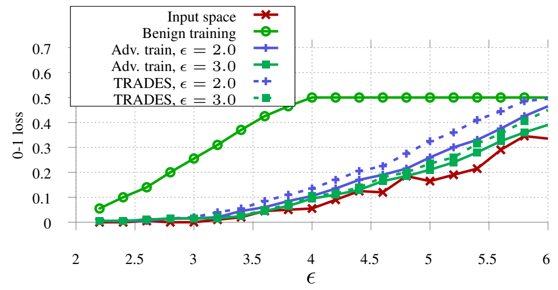

(b) Fashion MNIST

Figure 11. $0-1$ Loss: Robustness of the representation obtained from the *second ReLU layer* of a 3-layer FCNN using different training procedures.

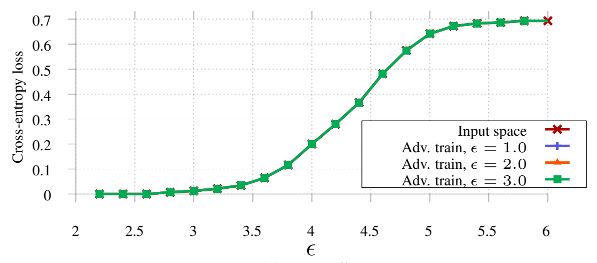

(a) MNIST

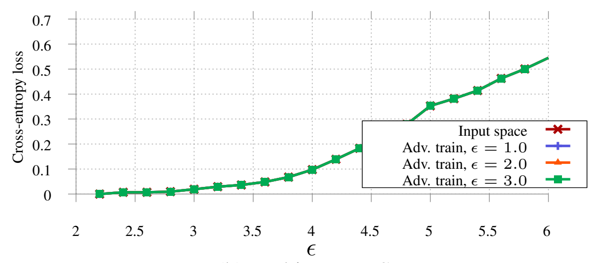

(b) Fashion MNIST

Figure 12. Robustness of the representation obtained from the *first linear layer* of a 4-layer CNN using different training procedures.